Journal of
Materials Chemistry B

PAPER

View Article Online
View Journal | View Issue

Cite this: *J. Mater. Chem. B*, 2016, **4**, 3086

Microfluidically fabricated pH-responsive anionic amphiphilic microgels for drug release

B. Lu,[a] M. D. Tarn,[a] N. Pamme*[a] and T. K. Georgiou*[b]

Received 13th November 2015,
Accepted 26th December 2015

DOI: 10.1039/c5tb02378e

www.rsc.org/MaterialsB

Amphiphilic microgels of different composition based on the hydrophilic, pH-responsive acrylic acid (AA) and the hydrophobic, non-ionic *n*-butyl acrylate (BuA) were synthesised using a lab-on-a-chip device. Hydrophobic droplets were generated *via* a microfluidic platform that contained a protected form of AA, BuA, the hydrophobic crosslinker, ethylene glycol dimethacrylate (EGDMA), and a free radical initiator in an organic solvent. These hydrophobic droplets were photopolymerised within the microfluidic channels and subsequently hydrolysed, enabling an integrated platform for the rapid, automated, and *in situ* production of anionic amphiphilic microgels. The amphiphilic microgels did not feature the conventional core–shell structure but were instead based on random amphiphilic copolymers of AA and BuA and hydrophobic crosslinks. Due to their amphiphilic nature they were able to encapsulate and deliver both hydrophobic and hydrophilic moieties. The model drug delivery and the swelling ability of the microgels were influenced by the pH of the surrounding aqueous solution and the hydrophobic content of the microgels.

Introduction

Three-dimensionally crosslinked polymer networks with sizes ranging from 0.1 to 100 μm are often referred to as gel particles or microgels. These particles, which are usually dispersed in a solvent, have many exciting biomedical applications such as in drug delivery,[1–10] tissue engineering,[2] and biosensing,[11] as well as applications in the oil industry,[12] organic dye removal,[13,14] coatings[15] and the food industry.[16] If the microgels are hydrophilic then they can be dispersed in aqueous solvents, while if they are hydrophobic they are usually called latex particles and cannot be dispersed in aqueous media. Gel particles/microgels that are amphiphilic, in other words containing both hydrophilic and hydrophobic groups, offer the advantage that they can be dispersed in both aqueous and non-aqueous media as well as encapsulate and release both hydrophilic and hydrophobic moieties.

Amphiphilic microgels, though, are challenging to fabricate because most of the production methods, such as conventional emulsion templating, involve the formation of droplets in an immiscible continuous phase, as shown in Fig. 1. The droplets contain pre-gels or polymerisable reagents that are later reacted to form the microgel. Thus, when fabricating hydrophilic microgels, the hydrophilic reagents are dispersed in aqueous droplets

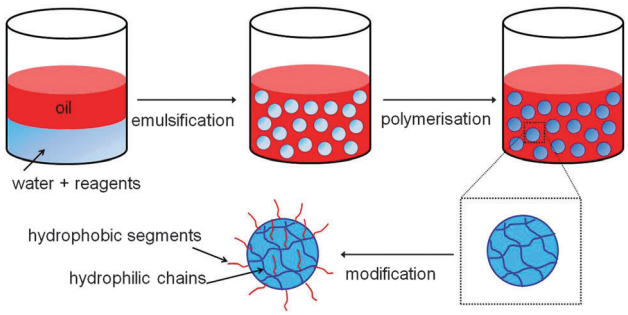

Fig. 1 Schematic illustration of the most common approach to amphiphilic microgel production *via* emulsion templating and post-modification of the microgel. The hydrophobic and hydrophilic moieties are coloured in red and blue, respectively.

while the continuous phase (CP) is an organic solvent/oil in which the reagents have reduced or no solubility. However, if the CP is aqueous then the hydrophilic reagent will diffuse from the droplets to the surrounding CP, and *vice versa*. Likewise, if the CP is based on oil or an organic solvent, then hydrophobic reagents would diffuse from the droplets to the CP. Thus, amphiphilic microgels are usually prepared using post-modifications[1,4,7,17–21] and/or multi-step procedures.[6,22] Typically, hydrophilic microgels are initially fabricated and then modified to produce amphiphilic microgels by covalently or electrostatically binding amphiphilic or hydrophobic moieties.[1,4,7,18–21] However this results in a "core–shell" microgel structure since the attachment happens mostly on the outer area/surface of the microgel

[a] *Department of Chemistry, University of Hull, HU6 7RX, Hull, UK. E-mail: n.pamme@hull.ac.uk*
[b] *Department of Materials, Imperial College London, SW7 2AZ, London, UK. E-mail: t.georgiou@imperial.ac.uk*

and the hydrophobic groups are never within the elastic chain (the chain between the crosslinks) but instead grafted on the chain.

The application of microfluidic platforms[23] for the production of gel particles offers the advantages of (i) generating droplets,[24,25] and consequently microgels, of narrower size distribution and (ii) the ability to tailor the size of the droplets/microgels by varying the applied flow rates of the droplet dispersed phase (DP) and the CP.[16,26–29] Furthermore, when using a microfluidic device, reactions can be performed on the droplets directly within the microchannels, or immediately following off-chip collection of the droplets, thereby enabling the polymerisation of some relatively unstable and easily hydrolysed reagents. For example, (meth)acrylic monomers tend to hydrolyse to (meth)acrylic acid when in contact with water,[30] so they cannot easily be dispersed in water or be polymerised in water to produce amphiphilic microgels.

Our previous study[31] was, to the best of our knowledge, the first in which amphiphilic microgels were produced using a lab-on-a-chip device. Specifically, amphiphilic microgels based on a hydrophilic monomer and a hydrophobic crosslinker were fabricated by the formation of precursor droplets within the microchannels and their subsequent collection and off-chip polymerisation. In this study, we have designed a new microfluidic chip with a long and deep serpentine channel that allowed the droplets to travel within the chip itself for a longer period of time, enabling their rapid and *in situ* polymerisation in an automated fashion. This new platform offers the advantage of ensuring even narrower size distributions of the droplets without risking their coalescence or getting destabilisation. In our previous study, anionic amphiphilic microgels of varying crosslinking densities, which was proportional to the hydrophobic content, were fabricated and the effect on the ability of the microgels to swell was investigated, in addition to their capacity to encapsulate and release hydrophobic and hydrophilic moieties used as models drugs.[31]

In the present study the crosslinking density was kept constant and a hydrophobic monomer (*n*-butyl acrylate, BuA) was introduced on the elastic chain (the chain between the crosslinks) in order to allow the hydrophobic content to be systematically varied without changing crosslinking density. The crosslinker, ethylene glycol dimethacrylate (EGDMA), was kept the same as in our previous work, as was the hydrophilic monomer, acrylic acid (AA). Since acrylic acid is not soluble in the chloroform dispersed phase into which the BuA and EGDMA were dissolved, the same approach as used in the previous study was employed by which a protected form of AA, specifically tetrahydropyranyl acrylate (THPA), was synthesised in-house and incorporated into the DP for polymerisation. The resulting THPA–BuA–EGDMA microgels were then hydrolysed to deprotect the AA units and thus form anionic amphiphilic AA–BuA–EGDMA microgels. Microgels of varying hydrophobic/hydrophilic (BuA/AA) ratio but with the same crosslinking density were fabricated. The pH responsiveness of the AA based microgels was evaluated by studying their swelling in different aqueous pH solutions. Finally, to demonstrate the amphiphilic nature of the microgels and their potential for drug delivery, the encapsulation and release of both hydrophobic and hydrophilic moieties was investigated using Sudan I and Trypan Blue, respectively, as model drugs.

Experimental

Materials and methods

Acrylic acid (AA, 99%), *n*-butyl acrylate (BuA, 99%), 2,3-dihydro-2*H*-pyran (DHP, 99%), ethylene glycol dimethacrylate (EGDMA, crosslinker), sodium dodecyl sulfate (SDS), 2,2-diphenyl-1-picrylhydrazyl hydrate (DPPH, free radical inhibitor, 99%), 1-hydroxycyclohexyl phenyl ketone (HCPK, 99%, free radical initiator), Sudan I, Trypan Blue, phenothiazine (98%, free radical inhibitor), sulphuric acid, sodium bicarbonate ($NaHCO_3$), sodium sulphate (Na_2SO_4), hydrochloric acid, sodium hydroxide and basic alumina were purchased from Sigma-Aldrich (Dorset, UK). BuA and EGDMA were passed through a basic alumina column to remove the free radical initiator prior to use. The organic solvent used to prepare the hydrophobic droplets was chloroform (99%), and was purchased from Fisher Scientific (Loughborough, UK). The chemical structures of the main reagents used for microgel fabrication (AA, BuA and EGDMA), including the in-house synthesised monomer (THPA, synthesis described below) are shown in Fig. 2.

Synthesis of protected acrylic acid monomer, tetrahydropyranyl acrylate (THPA). The synthesis of THPA was similar to the previously described synthesis of tetrahydropyranyl (meth)acrylate.[31–36] In a 500 mL three neck round bottom flask that contained 1 g of phenothiazine (free radical inhibitor) and 125 mL of DHP (116.25 g, 1.38 mol), 20 drops of a 50% v/v sulphuric acid solution in water were added drop-wise. The solution should change from colourless to brown. Following this, a mixture of 125 mL DHP (116.25 g, 1.38 mol), 94.6 mL AA (99.4 g, 1.38 mol) and 1 g phenothiazine (using a dropping funnel) was added and the round bottom flask was placed in an oil bath. The mixture was then left to react overnight at 50 °C.

The next day, once the mixture had cooled, 10 g of $NaHCO_3$ and 40 g of Na_2SO_4 were added and allowed to stir for 2–3 h. The solids were then filtered out and the monomer mixture was passed through two basic alumina columns (to remove the un-reacted AA, the THPMA monomer yield was ~60%). The removal of AA was confirmed by ^1H NMR. A free radical inhibitor, DPPH, was added into the THPA monomer, which was then stored in the fridge. The THPA was distilled under vacuum prior to use.

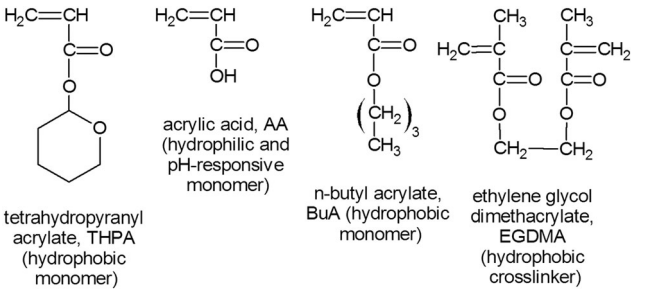

Fig. 2 Chemical structures of the monomers and crosslinker.

Fabrication of microgels

Microfluidic chip fabrication and setup. The microfluidic chip used for droplet formation and polymerisation consisted of three distinct regions: (i) a flow focusing section for the generation of THPA–BuA–EGDMA containing droplets, (ii) a short, shallow serpentine mixing channel that allowed rapid mixing of the droplet components, and (iii) a long, wide and deep serpentine channel for UV irradiation of the droplets (Fig. 3a). The chip was composed of a top layer and a bottom layer, and was fabricated from glass (B270 glass, Telic, CA, USA) using conventional photolithography and wet etching techniques.[37] The design in the top layer was etched to a depth of 10 μm and featured the flow focusing droplet generation and short serpentine mixing section that had channel widths of 30 μm, and a long, wide serpentine channel that had a channel width of 720 μm and a length of 188.35 cm. The bottom layer featured only the long, wide serpentine channel, as a mirror image to the design on the top later, that was etched to a width of 800 μm and a depth of 50 μm. The two layers were aligned and thermally bonded in a furnace at 585 °C for 3 h, yielding a final depth for the long and wide serpentine channel of 60 μm (Fig. 3b). Fused silica capillaries (150 μm i.d., 363 μm o.d., CM Scientific, UK) were glued into the inlet and outlet holes and connected to 500 μL glass syringes (SGE, Sigma-Aldrich, UK) *via* syringe adaptors (Kinesis, UK) (Fig. 3b). Two syringe pumps (PHD2000, Harvard Apparatus, UK) were used to control the flow rates of the CP and DP between 0.5 μL min^{-1} and 5 μL min^{-1}. The syringes and the droplet generation section on the chip were covered with aluminium foil in order to prevent the reagents from polymerising prior to droplet formation. Photopolymerisation was achieved using a 12 W, 365 nm UV light source (XX-15S, Ultra-Violet Products Ltd., UK). The entire setup was covered with a thick black cloth to in order to protect users from UV light.

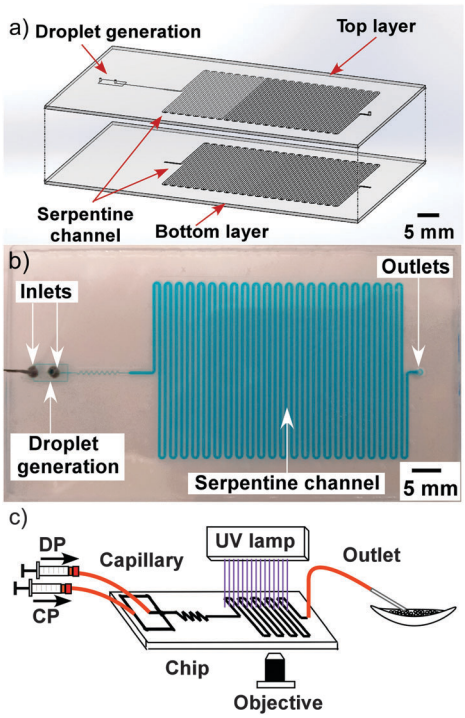

Fig. 3 (a) Exploded schematic of the microfluidic device, featuring a flow focusing junction and a long serpentine channel in the top layer (10 μm deep, 30 μm wide), and the serpentine channel (50 μm deep, 800 μm wide, 188.35 cm long) mirrored in the bottom layer. (b) Photograph of the microfluidic chip fabricated in glass, with blue dye used to visualise the microchannels. (c) Schematic showing the principle of droplet generation *via in situ* UV polymerisation to form microgels.

Videos and images of on-chip droplet generation were obtained using a colour CCD camera (MTV-63V1N, Mintron, Taiwan) attached to an inverted microscope (Eclipse Ti, Nikon, UK), with images captured *via* WinDVD Creator 2 (Corel Ltd, UK) software. Collected microgels were observed either on the same microscope setup, or using a second setup consisting of an upright microscope (BH-2, Olympus, UK), a CCD camera (INFINITYlite, Lumenera) and capture software (Studio Capture, Mettler-Toledo, Inc.). ImageJ freeware was used for the analysis of droplet size and colour intensity.

Formation of droplets and polymerisation of microgels. The DP was based on chloroform containing THPA, BuA and EGDMA with varying molar ratios of THPA and BuA (though the total concentration of the reagents was always 30 wt% and thus the monomer crosslinker ratio was always 70 : 4 THPA/BuA : EGDMA), and 4 wt% of HCPK (free radical photoinitiator). The CP was an aqueous solution of 0.1 wt% SDS, with the concentration of SDS being below the critical micelle concentration.[38] During droplet generation optimisation studies, the flow rate of the CP was varied from 0.5 μL min^{-1} to 5 μL min^{-1}, while the DP flow rate was held at 0.5 μL min^{-1}. Later microgel fabrication was performed at CP and DP flow rates of 2 μL min^{-1} and 0.5 μL min^{-1}, respectively. These flow rates allowed the droplets to be UV irradiated for 30 min as they passed through the serpentine channel, forming the microgels. One THPA–EGDMA microgel and three THPA–BuA–EGDMA microgels of differing compositions were formed, with molar ratios of 75 : 0, 49 : 21, 35 : 35, and 21 : 49 THPA : BuA, respectively. The polymerised microgels were collected off-chip and then hydrolysed in a solution of 0.01 M HCl solution (pH 2) overnight to produce pH responsive AA–BuA–EGDMA microgels. The hydrolysis was confirmed with FTIR.

Swelling studies in different pH environments

Aqueous solutions of NaOH (1 M) and HCl (1 M) were used to vary the pH of the solution that the AA–BuA–EGDMA microgels were suspended in, from pH 1 to pH 14. These tests were performed in order to study the responsiveness of the microgel particles. The microgels were photographed using the colour CCD camera and microscope setups described previously, with ImageJ used for image analysis. The extent of swelling and shrinking (relative size) was calculated by dividing the microgel diameter at a given pH by their original diameter measured at pH 7.

pK_a determination

The pK_a values of the three synthesised AA–BuA–EGDMA microgels were determined by potentiometric titration. Specifically,

0.02 g of each microgel was dispersed in water, and 1 M NaOH added to increase the pH above 11. The titration was performed by adding 0.05 mL aliquots of 0.1 M HCl and measuring the pH after each addition.

Dye encapsulation and release studies

Two types of dye, acting as model drugs, were encapsulated in the microgels *via* two different methodologies to determine the capability of the microgels to encapsulate and release both hydrophilic and hydrophobic moieties. 1 wt% hydrophobic Sudan I was mixed into the DP prior to droplet formation, hence the dye was already present inside the microgel following droplet generation and polymerisation. 1 wt% hydrophilic Trypan Blue was loaded into already polymerised AA containing microgels in a pH 14 solution by diffusion with sonication for 30 min, before removing the microgels by pipette, adding them to a microscope slide and removing any excess solution. The chemical structures of both dyes are shown in Fig. 4. The model drug release was monitored using the colour camera of the microscopes. In particular, the change in microgel colour intensity over time. Images were taken at regular time intervals (every 1 min or 5 min depending on the rate of release). ImageJ freeware was used for the analysis of the colour intensity.

Results and discussion

Droplet generation and polymerisation

The influence of flow rate on droplet size in the new microfluidic chip design was first investigated by increasing the flow rate of the CP from 0.5 μL min^{-1} to 5 μL min^{-1}, while the DP flow rate was held at 0.5 μL min^{-1}, allowing droplet diameters to be controlled between 8 μm (volume of 0.3 pL) and 18 μm (3.1 pL) (CV typical ~9%) (Fig. 5). This enabled far smaller monodisperse droplets to be produced compared to the microfluidic chip design used in the previous study,[31] in which droplets of ~130 μm could be generated with similar CVs to those shown here, while smaller droplets yielded much larger CVs. The smaller droplet sizes in this study were achieved as a result of the much shallower and thinner channel dimensions in the flow focusing section of the chip (Fig. 6a). For amphiphilic microgel fabrication, the flow rates of the CP and DP were 2 μL min^{-1} and 0.5 μL min^{-1}, respectively, yielding droplets with a volume of 3.1 pL (CV 7%). The droplets then passed through the short serpentine mixing section, with the same dimensions as the flow focusing channels due to their being in the same layer of the fabricated chip, which allowed rapid mixing of the monomers (THPA and BuA) and crosslinker (EGDMA) inside the droplets. Following this, the droplets passed from the 10 μm deep channel (Fig. 6b) to the 60 μm deep serpentine channel (Fig. 6c), where they went from being pancake shaped in the narrow channels to spherical in the deeper channel. Interestingly, as the droplets traversed this shallow serpentine channel they were observed to experience inertial forces,[39,40] which focused them to the outer edges of the channel before they entered the deeper channel region (Fig. 6c).

The dimensions of the large serpentine channel meant that, at the applied flow rates, the droplets were polymerised to

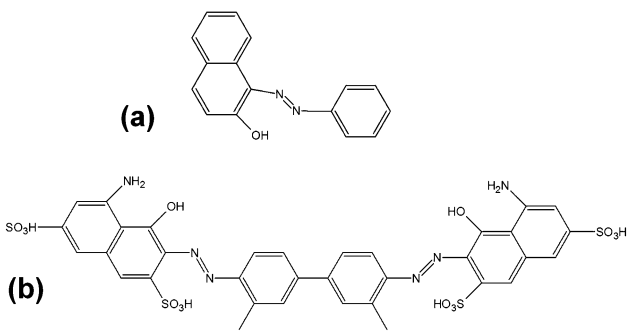

Fig. 4 Chemical structures of (a) hydrophobic Sudan I dye, and (b) hydrophilic Trypan Blue dye.

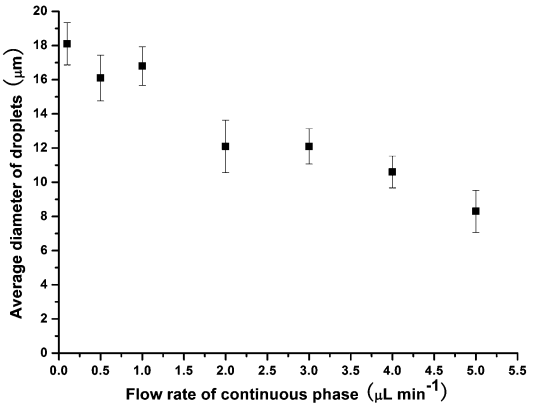

Fig. 5 Control of droplet size by varying the flow rate of the aqueous continuous phase, with the dispersed phase flow rate held constant at 0.5 μL min^{-1}.

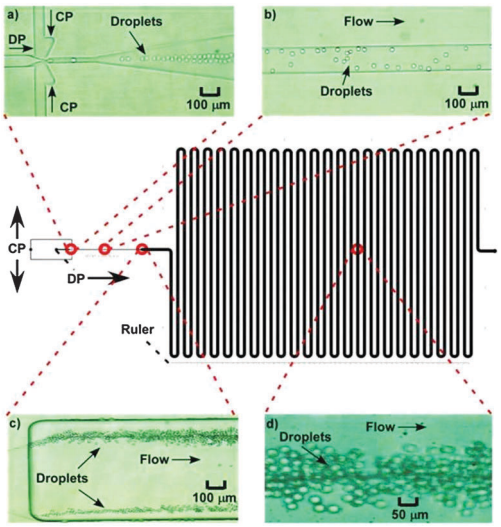

Fig. 6 Photographs of droplets (a) being generated at the flow focusing junction, (b) in the 10 μm deep channel, (c) entering the 60 μm deep serpentine channel, and (d) inside the serpentine channel where they would undergo UV polymerisation.

THPA–BuA–EGDMA microgels for 30 min as they passed through it (Fig. 6d). These features offered further improvement over the previous chip design[31] in which the generated droplets could not be polymerised on-chip due to the extremely short residence time, while the droplets also remained flattened in the chip and only became spherical when collected in a dish for off-chip polymerisation (30 min). Thus, the new chip design and setup enabled integrated, *in situ* polymerisation of small, monodisperse, spherical microgels, in an essentially automated fashion; a scenario that was not possible with the previous chip setup. This also allowed better microgel size distribution and more accurate polymerisation times without risking the droplets being destabilised and any monomer leaking out of the droplets prior to polymerisation.

The polymerised microgels were collected from the chip outlet, and the THPA groups were deprotected by adding the microgels to a solution of HCl (pH 2) to form AA groups by hydrolysis. The resulting amphiphilic AA–BuA–EGDMA microgels consisted of a hydrophilic AA, hydrophobic BuA and hydrophobic EGDMA crosslinked internal network, whose ratios could be altered by varying the relative amounts of each component in the precursor DP solution.

Microgel fabrication and pH responsiveness studies

Three types of amphiphilic AA–BuA–EDGMA microgels of different compositions, in addition to a AA–EGDMA homopolymer microgel, were successfully fabricated *via* the microfluidic approach described above. Specifically, the four populations contained different monomer ratios (AA : BuA) but the same crosslinking density (monomer : EGDMA 70 : 4), yielding final AA : BuA : EGDMA ratios of 41 : 29 : 4, 35 : 35 : 4, 21 : 49 : 4, and 70 : 0 : 4 (*i.e.* 70 : 4 AA : EGDMA), were produced. Thus, the hydrophobic content was only varied by altering the hydrophilic (AA) : hydrophobic (BuA) monomer molar ratio.

The pH responsiveness, in terms of swelling and shrinking, of the microgels was studied by measuring the size of the microgels at different pH values. As can be observed in Fig. 7, the size of the microgels increased with the increase in the pH of the solution, as was expected. The AA units at high pH become ionised due to deprotonation and thus more hydrophilic. This allows more water to enter the microgel, allowing it to swell. Furthermore, the anionic charges of the AA groups repel each other, forcing polymer chains to extend more and so cause the microgel to swell. This has been observed previously for (meth)acrylic acid containing microgels[4,5,31,41] and macrogels.[33–35,42–44] Note that the size of the microgels at very basic pH reduces because of increased ionic strength due to the increased NaOH concentration, as has also been observed in macrogels[34,35] and microgels.[31]

When comparing the four different microgels it can be clearly observed that the size change, and thus the degree of swelling, was affected by the hydrophobic content but not at all pH values. At low pH, the AA units became protonated and non-ionised, while the hydrophobic content did not have an effect on the swelling ratio because the whole elastic chain (polymer chain between the crosslinks) was in a collapsed state. For example,

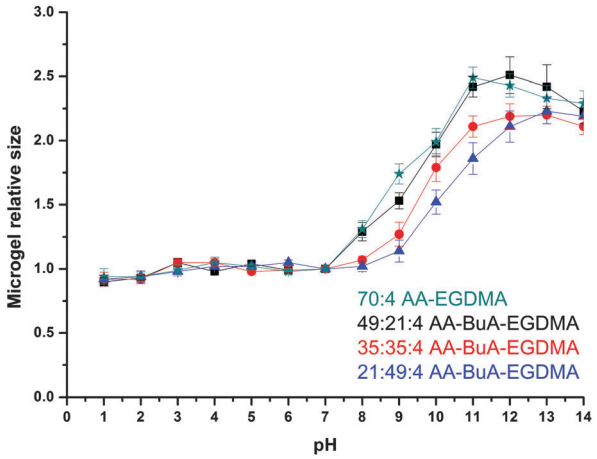

Fig. 7 Swelling ratios of the AA–BuA–EGDMA microgels and the AA–EGDMA microgel at different pH values. Microgels formed with AA : BuA : EGDMA molar ratios of 70 : 0 : 4, 21 : 49 : 4, 35 : 35 : 4, 49 : 21 : 4 are represented as green stars, blue triangles, red circles and black squares, respectively.

at pH 7 the actual size/diameters of all microgels ranged from 17.9 to 18.6 μm. When exposed to high pHs the microgels with lesser hydrophobic content (*i.e.* lower BuA/AA ratio) swelled more since they were more anionic charges that forced the elastic chains to extend more as well as to repel each other, and thus force the whole microgel structure to swell. For example at pH 9 the diameter of the microgels increased from 21.3 to 31.0 μm as the AA content increased in the microgel. This was expected and similarly observed in macrogels.[34,35,45–50]

pK_as of amphiphilic microgels

The hydrophobic content also influenced the pK_a of the microgels, which were determined by potentiometric titration. Specifically, when the hydrophobic BuA content was varied between 0% (AA : BuA : EGDMA 70 : 0 : 4), 41% (21 : 49 : 4), 50% (35 : 35 : 4) and 59% (49 : 21 : 4), based on the molar ratio of BuA (BuA/(BuA + AA) × 100%), the pK_a values increased from 6.1 to 6.2, 6.4 and 6.6, respectively. Thus, the effective pK_a values decreased as the AA content of the amphiphilic microgels increased, or equivalently, as the BuA content decreased. In other words, AA became a stronger acid as the microgels became less hydrophobic. This is because a decrease in the BuA content caused an increase in the hydrophilicity and in the dielectric constant of the microgels, rendering ionisation easier, which resulted in the lowering of the effective pK_a.[51] This has been similarly observed in anionic (meth)acrylic acid based amphiphilic macrogels[34,35,45] and the reverse trend has been seen in amino (base) containing amphiphilic macrogels (pK_a decreased with increasing hydrophobic content).[46,49,50]

Dye encapsulation and release studies

Having established that the microfluidically fabricated microgels were pH responsive, their ability to encapsulate and release both hydrophilic and hydrophobic moieties was examined. The intent was two-fold: (i) to prove the amphiphilic nature of the anionic AA microgels, and (ii) to determine their potential as

delivery vehicles for drugs of varying hydrophobicity/hydrophilicity, similar to macrogels.[52,53] A hydrophobic dye (Sudan I) and a hydrophilic dye (Trypan Blue) were employed as model drugs for these studies, with their release triggered by swelling of the microgels.

Hydrophobic dye – Sudan I. Sudan I (Fig. 4a) was encapsulated into the microgels during the on-chip polymerisation step. The Sudan I was mixed into the DP with the monomer and cross-linker reagents (THPA, BuA, EGDMA), such that when the precursor droplets were formed and polymerised they already contained the dye. Fig. 8a shows a newly prepared AA_{49}-*co*-BuA_{21}-*co*-$EGDMA_4$ microgel with the Sudan I encapsulated inside, suspended in a pH 7 solution. When a basic solution (pH 14) was added the microgel immediately swelled and started to release the dye. The progress could be observed as a colour change over time, from immediately after addition of the pH 14 solution (Fig. 8b) to 30 min later (Fig. 8c). As described in the previous section, upon addition of the basic solution the AA units became hydrophilic and prone to internal electrostatic repulsion between deprotonated AA groups, thus causing the polymer chains to extend and forcing the microgel to swell to the extent that the microgel could no longer retain the hydrophobic dye, resulting in a loss in colour intensity over time.

The dye release rate was further investigated for each of the four types of microgel, and the results are shown in Fig. 9. Each of the microgels was able to encapsulate and release the dye, but there was a clear influence of the hydrophobic content on the release rate. In particular, by increasing the hydrophobic monomer (BuA) molar ratio content from 0% (70 : 0 : 4 AA : Bu : EGDMA) to 70% (21 : 49 : 4), the rate of release of the hydrophobic dye decreased. This was expected since the hydrophobic components of the microgel retained the hydrophobic dye in the microgel structure to a greater extent, as a result of hydrophobic interactions. Furthermore, the fact that the microgels with a higher hydrophobic content swelled less would also have an influence as it would slow the diffusion of the dye through the microgel, thus reducing the release rate.

Hydrophilic dye – Trypan Blue. The encapsulation and release of the hydrophilic dye, Trypan Blue (Fig. 4b), was also investigated. Fig. 10a shows an AA_{49}-*co*-BuA_{21}-*co*-$EGDMA_4$ microgel immediately following Trypan Blue encapsulation in pH 14 solution (as described in the Experimental section) and subsequent washing and suspension in pH 7 solution. Fig. 10b and c show the same microgel after 5 and 30 minutes following suspension in pH 7 solution, respectively. The gradual release

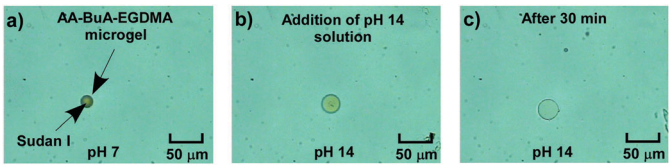

Fig. 8 (a) AA_{49}-*co*-BuA_{21}-*co*-$EGDMA_4$ microgel with hydrophobic Sudan I dye encapsulated inside at pH 7. (b) The same microgel immediately after addition of pH 14 solution, and (c) 30 min after addition of pH 14 solution.

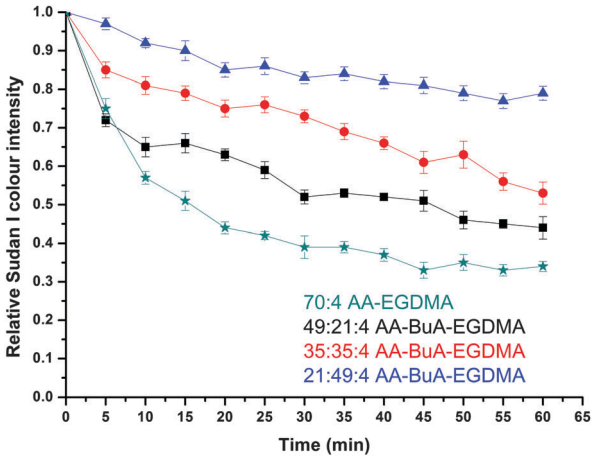

Fig. 9 Hydrophobic drug release in basic (>pH 11) conditions. The plots show the relative Sudan I colour intensity *versus* time for four types of AA–BuA–EGDMA microgels with different AA/BuA molar ratios. Green stars, black squares, red circles and blue triangles represent the microgels with 70 : 0 : 4, 49 : 21 : 4, 35 : 35 : 4 and 21 : 49 : 4 AA : BuA : EGDMA molar ratios, respectively.

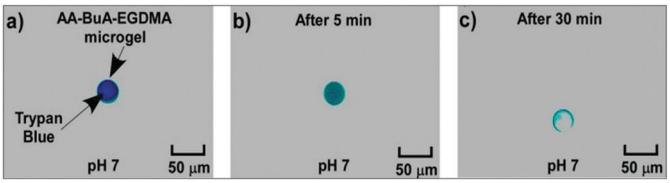

Fig. 10 Hydrophilic Trypan Blue encapsulation in, and release from, a AA_{49}-*co*-BuA_{21}-*co*-$EGDMA_4$ microgel (a) immediately following encapsulation and suspension in pH 7 solution, (b) 5 min later, and (c) 30 min after suspension in pH 7 solution.

of the hydrophilic Trypan Blue in the surrounding water can be observed based on intensity of the blue colour inside the microgel, which faded with time.

The release of the hydrophilic dye was further investigated over time for all four AA–BuA–EGDMA microgels in neutral (pH ~7, Fig. 11) and basic (pH 11, Fig. 12) solutions. Two main observations can be made from the acquired data. Firstly, that by increasing the hydrophobic content (greater ratio of BuA), the hydrophilic dye release rate was decreased, as was expected and as had also been observed for the hydrophobic dye. This was as a result of the microgels with higher hydrophobic content swelling to a lesser extent, the pore/mesh size being smaller, and the fact that the dye could not diffuse out of the microgel as fast, compared to those with lower hydrophobic content. The second observation was that the dye release was much faster at pH 11 (Fig. 12) than pH 7 (Fig. 11). This was observed for all four varieties of microgels, and had similarly occurred in our previous studies,[31] since more basic conditions yielded greater swelling (Fig. 7) due to the AA ionisation.

When comparing the hydrophobic Sudan I release to that of Trypan Blue from the amphiphilic microgels, the latter demonstrated much faster release characteristics for all four microgels at basic pH. For example, it took more than 40 min for the

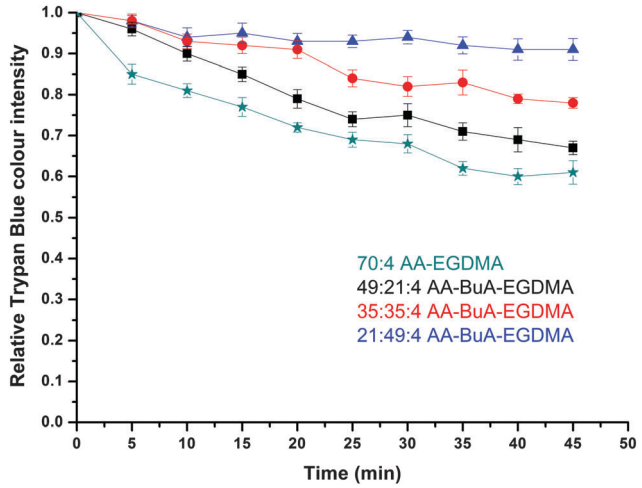

Fig. 11 Hydrophilic dye release in neutral pH solution (~pH 7). The plots show the relative Trypan Blue colour intensity *versus* time for each variation of the AA–BuA–EGDMA microgels. Green stars, black squares, red circles and blue triangles represent microgels with 70 : 0 : 4, 49 : 21 : 4, 35 : 35 : 4 and 21 : 49 : 4 AA : BuA : EGDMA molar ratios, respectively.

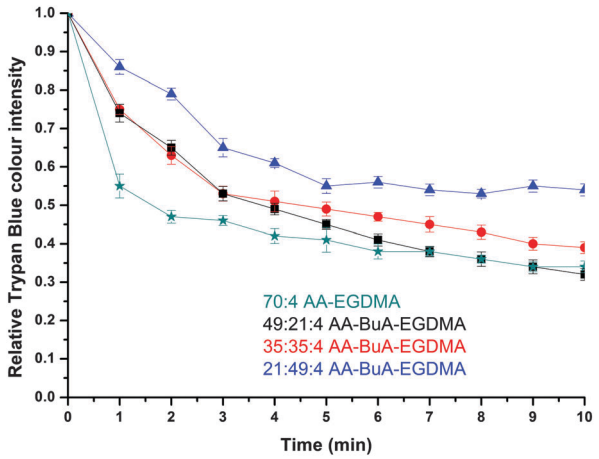

Fig. 12 Hydrophilic dye release in basic pH solution (~pH 11). The plots show the relative Trypan Blue colour intensity *versus* time for all AA–BuA–EGDMA microgels with different AA–BuA ratios and the AA homopolymer, AA–EGDMA. Green stars, black squares, red circles and blue triangles represent the microgels with 70 : 4, 49 : 21 : 4, 35 : 35 : 4 and 21 : 49 : 4 AA : BuA : EGDMA molar ratios, respectively.

release of hydrophobic Sudan I from AA_{49}-*co*-$BuMA_{21}$-*co*-$EGDMA_4$ microgels at basic pH to reach 50% of the relative colour intensity (compared to the initial intensity), while this level was reached in only 5 min during hydrophilic Trypan Blue release. This can be attributed to two factors: (i) the difficulty of the hydrophobic dye to diffuse into an aqueous environment compared to the hydrophilic dye, and (ii) the fact that the hydrophobic domains of the microgels would retain for longer the hydrophobic dye through hydrophobic interactions. It should be noted that this was observed in our previous study on off-chip polymerised AA–EGDMA microgels as well.[31]

In summary, the AA–BuA–EGDMA microgels were able to encapsulate and deliver both hydrophobic and hydrophilic dyes, and it has been demonstrated that the release rate can be tailored by adjusting the hydrophobic content of the amphiphilic microgels, which shows promise for their use in future drug delivery applications.

Conclusions

Amphiphilic microgels based on hydrophilic, ionisable acrylic acid (AA), hydrophobic, non-ionic *n*-butyl acrylate (BuA) and the hydrophobic crosslinker ethylene glycol dimethacrylate (EGDMA) were successfully fabricated in a lab-on-a-chip device *via in situ* generation and direct UV polymerisation of spherical precursor droplets in an expanded serpentine channel. The use of such an integrated microfluidic platform enabled the systematic variation of the amphiphilic nature of the microgels by varying the hydrophilic/hydrophobic monomer ratio, while maintaining the crosslinking density, producing microgels with narrower size distributions than those prepared by conventional methods. The microgels were pH responsive; by increasing the pH of the surrounding environment the microgels swelled due to ionisation of the AA units and the resultant electrostatic repulsion between the polymer chains inside the gel particles. Furthermore, it was demonstrated that the extent of swelling could be controlled by tailoring the hydrophobic content, as the microgel swelling was found to decrease by increasing the hydrophobic BuA content. Finally, the encapsulation and release of two model drugs, one hydrophobic dye and one hydrophilic dye, were investigated, and highlighted the amphiphilic nature of the microgels. The release was influenced by both the hydrophobic content of the microgels and the pH of the surrounding solution. In particular, by increasing the hydrophilic content of the microgels and suspending them in a more basic solution, the release of the dyes was accelerated. These properties and initial trials show great potential for the use of on-chip generated amphiphilic microgels for the encapsulation and triggered release of hydrophilic and hydrophobic payloads, particularly with a view to drug delivery applications.

Acknowledgements

University of Hull is thanked for funding Mr Lu's PhD studentship. Dr Stephen Clark is thanked for fabrication of the microfluidic devices.

Notes and references

1 V. Alakhov, G. Pietrzynski, K. Patel, A. Kabanov, L. Bromberg and T. A. Hatton, *J. Pharm. Pharmacol.*, 2004, **56**, 1233–1241.
2 Y. Jiang, J. Chen, C. Deng, E. J. Suuronen and Z. Zhong, *Biomaterials*, 2014, **35**, 4969–4985.
3 Y. Gao, A. Ahiabu and M. J. Serpe, *ACS Appl. Mater. Interfaces*, 2014, **6**, 13749–13756.
4 L. Bromberg, M. Temchenko and T. A. Hatton, *Langmuir*, 2002, **18**, 4944–4952.
5 J. P. K. Tan and K. C. Tam, *J. Controlled Release*, 2007, **118**, 87–94.

6 W. C. Lee, Y. C. Li and I. M. Chu, *Macromol. Biosci.*, 2006, **6**, 846–854.
7 L. Li, C. Cheng, M. P. Schürings, X. Zhu and A. Pich, *Polymer*, 2012, **53**, 3117–3123.
8 M. Dadsetan, K. E. Taylor, C. Yong, Ž. Bajzer, L. Lu and M. J. Yaszemski, *Acta Biomater.*, 2013, **9**, 5438–5446.
9 H. Bysell, R. Månsson, P. Hansson and M. Malmsten, *Adv. Drug Delivery Rev.*, 2011, **63**, 1172–1185.
10 T. Trongsatitkul and B. M. Budhlall, *Polym. Chem.*, 2013, **4**, 1502–1516.
11 M. R. Islam, A. Ahiabu, X. Li and M. J. Serpe, *Sensors*, 2014, **14**, 8984–8995.
12 Y. Chen, Y. Bai, S. Chen, J. Jup, Y. Li, T. Wang and Q. Wang, *ACS Appl. Mater. Interfaces*, 2014, **6**, 13334–13338.
13 D. Parasuraman and M. J. Serpe, *ACS Appl. Mater. Interfaces*, 2011, **3**, 4714–4721.
14 D. Parasuraman and M. J. Serpe, *ACS Appl. Mater. Interfaces*, 2011, **3**, 2732–2737.
15 C. D. Sorrell, M. C. D. Carter and M. J. Serpe, *ACS Appl. Mater. Interfaces*, 2011, **3**, 1140–1147.
16 H. M. Shewan and J. R. Stokes, *J. Food Eng.*, 2013, **119**, 781–792.
17 R. Yin, X. Cha, X. Zhang and J. Shen, *Macromolecules*, 1990, **23**, 5158–5160.
18 L. Bromberg, M. Temchenko, G. D. Moeser and T. A. Hatton, *Langmuir*, 2004, **20**, 5683–5692.
19 X. Wang, X. Hou, Y. Wu and S. You, *J. Appl. Polym. Sci.*, 2009, **114**, 4042–4050.
20 H. Li, X. Cui, S. Shen and D. Hu, *J. Appl. Polym. Sci.*, 2011, **122**, 509–516.
21 H. Li, P. Zhang, L. Zhang, T. Zhou and D. Hu, *J. Mater. Chem.*, 2009, **19**, 4575–4586.
22 T. Zhou, H. Li, G. Liu, L. Zhang, D. Yao and D. Hu, *J. Appl. Polym. Sci.*, 2009, **114**, 4000–4010.
23 M. D. Tarn and N. Pamme, in *Elsevier Reference Module in Chemistry, Molecular Sciences and Chemical Engineering*, ed. J. Reedijk, Elsevier, Waltham, MA, 2013.
24 H. Song, D. L. Chen and R. F. Ismagilov, *Angew. Chem., Int. Ed.*, 2006, **45**, 7336–7356.
25 S.-Y. Teh, R. Lin, L.-H. Hung and A. P. Lee, *Lab Chip*, 2008, **8**, 198–220.
26 E. Tumarkin and E. Kumacheva, *Chem. Soc. Rev.*, 2009, **38**, 2161–2168.
27 S. Seiffert and D. A. Weitz, *Polymer*, 2010, **51**, 5883–5889.
28 W. J. Duncanson, T. Lin, A. R. Abate, S. Seiffert, R. K. Shah and D. A. Weitz, *Lab Chip*, 2012, **12**, 2135–2145.
29 S. Seiffert, *Angew. Chem., Int. Ed.*, 2013, **52**, 11462–11468.
30 P. Van De Watering, N. J. Zuidam, M. J. Van Steenbergen, O. A. G. J. Van Der Houwen, W. J. M. Underberg and W. E. Hennink, *Macromolecules*, 1998, **31**, 8063–8068.
31 B. Lu, M. D. Tarn, N. Pamme and T. K. Georgiou, *J. Mater. Chem. B*, 2015, **3**, 4524–4529.
32 S. N. Georgiades, M. Vamvakaki and C. S. Patrickios, *Macromolecules*, 2002, **35**, 4903–4911.
33 T. K. Georgiou, L. A. Phylactou and C. S. Patrickios, *Biomacromolecules*, 2006, **7**, 3505–3512.
34 G. Kali, T. K. Georgiou, B. Iván, C. S. Patrickios, E. Loizou, Y. Thomann and J. C. Tiller, *Langmuir*, 2007, **23**, 10746–10755.
35 G. Kali, T. K. Georgiou, B. Iván, C. S. Patrickios, E. Loizou, Y. Thomann and J. C. Tiller, *Macromolecules*, 2007, **40**, 2192–2200.
36 K. S. Pafiti, Z. Philippou, E. Loizou, L. Porcar and C. S. Patrickios, *Macromolecules*, 2011, **44**, 5352–5362.
37 T. McCreedy, *Anal. Chim. Acta*, 2001, **427**, 39–43.
38 A. Pal and S. Chaudhary, *Fluid Phase Equilib.*, 2014, **372**, 100–104.
39 D. Di Carlo, D. Irimia, R. G. Tompkins and M. Toner, *Proc. Natl. Acad. Sci. U. S. A.*, 2007, **104**, 18892–18897.
40 D. Di Carlo, *Lab Chip*, 2009, **9**, 3038–3046.
41 G. M. Eichenbaum, P. F. Kiser, A. V. Dobrynin, S. A. Simon and D. Needham, *Macromolecules*, 1999, **32**, 4867–4878.
42 G. Kali and B. Iván, *Macromol. Chem. Phys.*, 2015, **216**, 605–613.
43 M. Haraszti, E. Tóth and B. Iván, *Chem. Mater.*, 2006, **18**, 4952–4958.
44 B. Iván, M. Haraszti, G. Erdödi, J. Scherble, R. Thomann and R. Mülhaupt, *Macromol. Symp.*, 2005, **227**, 265–273.
45 G. Kali, T. K. Georgiou, B. Iván and C. S. Patrickios, *J. Polym. Sci., Part A: Polym. Chem.*, 2009, **47**, 4289–4301.
46 T. K. Georgiou, C. S. Patrickios, P. W. Groh and B. Iván, *Macromolecules*, 2007, **40**, 2335–2343.
47 D. S. Achilleos, T. K. Georgiou and C. S. Patrickios, *Biomacromolecules*, 2006, **7**, 3396–3405.
48 A. I. Triftaridou, E. Loizou and C. S. Patrickios, *J. Polym. Sci., Part A: Polym. Chem.*, 2008, **46**, 4420–4432.
49 A. I. Triftaridou, S. C. Hadjiyannakou, M. Vamvakaki and C. S. Patrickios, *Macromolecules*, 2002, **35**, 2506–2513.
50 M. Vamvakaki and C. S. Patrickios, *Soft Matter*, 2008, **4**, 268.
51 O. E. Philippova, D. Hourdet, R. Audebert and A. R. Khokhlov, *Macromolecules*, 1997, **30**, 8278–8285.
52 P. Papaphilippou, M. Christodoulou, O. M. Marinica, A. Taculescu, L. Vekas, K. Chrissafis and T. Krasia-Christoforou, *ACS Appl. Mater. Interfaces*, 2012, **4**, 2139–2147.
53 N. Ghasdian, E. Church, A. P. Cottam, K. Hornsby, M. Y. Leung and T. K. Georgiou, *RSC Adv.*, 2013, **3**, 19070–19080.